A reciprocal variational approach to the two-body frictionless contact problem in elastodynamics

Joël. Bensoam[a]

[a] *Ircam, centre G. Pompidou, CNRS UMR 9912, Acoustic Instrumental Team, 1 place I. Stravinsky 75004 Paris, France*

Abstract

This paper deals with the theoretical and numerical treatment of the unilateral dynamic contact problem between two arbitrary elastic bodies without friction. In addition to the classical variational statement that arises from static problems, a dynamic contact condition is needed and found by adjusting the balance laws of physical quantities to the impenetrability condition. In the context of infinitesimal deformation, a reciprocal formulation is then used to reduce this well-posed problem to one involving Green functions defined only on contact surfaces. It is then often possible to approximate the system using considerably fewer unknowns than with finite difference algorithms. The ability of the method to predict the contact interaction between two elastic bodies, irrespective of the material constitution and geometry, is highlighted by analytical and numerical simulations.

Key words: contact problems, Signorini, frictionless contact, elastodynamics, Green functions, finite elements
PACS: 001

INTRODUCTION

The general problem of the equilibrium of a linear elastic body in contact with a frictionless foundation was formulated by Signorini [1] in 1933, who presented a more complete account of his theory in 1959 [2]. The first rigorous analysis of a class of Signorini problems was published by Fichera [3]. The work of Fichera represents the first treatment of the question of existence and uniqueness of variational inequalities arising from the minimization of the total potential energy functional on a convex constraint set that expresses the impenetrability between the body and the foundation.

Since then, the solution of the classical Signorini problem has been shown to be also the solution of a variational inequality that arises naturally from the principle of virtual work. See, for instance, Oden and Kikuchi [4] who laid the mathematical framework for a variational statement of the Signorini's problem and took up the question of existence and uniqueness of solutions. They also provided interpretations of weak solutions and discussed their relationship to the classical solution. As customary, saddle point theory (Lagrange multipliers) or penalty formulations were used to handle the contact constraint and finite element approximations were developed.

All these studies refer to static elasticity. Several authors have attempted to find the numerical solution of dynamic contact problems using finite element methods. Among them it is important to mention the work of Hughes et al. [5] who presented a finite element formulation for linearly elastic contact-impact problems valid for perfect frictionless condition on the contact surface. Careful procedures, compatible with waves propagation theory, were used to enforce linear momentum balance when the impact or the release of the contact nodes occurs.

Duvaut and Lions [6] have investigated the frictional dynamic contact problem with prescribed normal tractions on the contact boundary and were able to prove existence and uniqueness of solutions. The frictional effects are included in the variational formulation through a non-differentiable functional which represents the virtual power of the friction force. As a consequence of this non-differentiability, this dynamic contact problem provides also an example of physical system subject to a governing variational inequality. Applications of the finite element method to solve this variational inequality, including error estimates and adapted algorithms, were presented by Martins and Oden [7].

For unilateral contact, a variational inequality was also formulated, (e.g. Panagiotopoulos et al. [8, 9]). By discretizing this inequality with respect to time and using a finite element method, these authors also obtained a solution of the dynamic unilateral contact problem by solving a static problem at each time step. In this case, the contact conditions are devised on individual configurations without much regard to the temporal variation of the contact kinematic measures. Taylor and Papadopoulos [10], in the 90's, have shown that standard semi-discrete time integrators are unsuccessful in modeling the kinematic contact imposed on the interacting bodies during persistent con-

Email address: bensoam@ircam.fr (Joël. Bensoam)

tact.They have bypassed this difficulty by devising a special treatment of contact/release conditions. Since then, Laursen et al. [11] demonstrated that this dynamic kinematic condition guarantees the energy conservation for frictionless contact and proposed a formulation of dynamic contact problems which enables an exact algorithmic conservation of the linear momentum, angular momentum, and energy in finite element simulations. The ability of the formulation to produce accurate results where more traditional integration schemes fail is emphasized by their numerical simulations. Since then, many authors have been working on similar problems involving viscoelastic material (see for instance [12], [13] or [14]).

At this point is important to note that optimization theory adapted to dynamic contact problem needs, to give good numerical results, a dynamic condition that garantees the energy conservation. In the works mention above, this condition was postulated by the authors and a physical justification is still needed. This the major purpose of this article.

Usually, the variational inequality is obtained by adding a constraint to the classical equation of motion. Conversely, in the static case, Fichera [3] or Oden and Kikuchi [4] showed that equations of equilibrium with constraint can be derived from convex analysis and optimization theory (optimization of the potential energy here). It is then natural to seek a functional which is to the dynamic context what the total potential energy functional is to the static context.

The first section of this article show that the optimization of Hamilton's functional, on a constraint set that expresses the contact condition, can be used to obtain a formal statement of the two-body dynamic contact problem. In this framework, general non-linear programming methods are available and the problem can be formulated using saddle point theory where the Lagrange multiplier represents a contact pressure. To this purpose Taylor's procedure [10] is followed in the linear context.

Unfortunately, this statement is not sufficient since it is shown here that the energy balance must be considered to obtain a well-posed problem. In section 2, it is shown that the kinematic contact condition, derived from the static one by Taylor [10] and postulated by Laursen [11], is in fact a consequence of the continuum mechanic balance laws and represents the way the energy is dissipated during contact (that is to say under the impenetrability constraint).

Furthermore, in most of works, finite-difference methods are used to integrate the resulting equations of motion and can lead to numerical instabilities. In section 3, the reciprocal formulation, already used for static problems, is applied to the dynamic context. This method involves the inverse of the *elasticity operator* appearing in standard variational statements of linear problems. One of the advantages of this method is that the awkward problem of discontinuities, which arises in contact problems, is already treated in the definition of this operator usually called *Green function*. Moreover, since the contact pressure only occurs at the contact surface, the problem itself reduces to one involving functions defined only on this surface. It is then often possible to approximate the system using considerably fewer unknowns than with classical finite-difference methods. This algorithm was recently implemented in software written in C++. Contact between arbitrary bodies can now be performed in real-time synthesis at audio frequency 44100 Hz for a contact surface that involved dozens of candidate contact nodes. This performance is possible since the numerical computation can be split into two phases: computation of the kernels (Green and Poisson functions - only needed once), and real time iterative procedure and convolution to obtain the system's evolution.

Section 4 is concerned with two dynamic contact examples. The first one is a collision between two identical rods. In this one-dimensional case, an analytical solution is available and can be compared to numerical results. The second example exhibits nonlinear characteristics in the three-dimensional contact between two disk-shaped elastic bodies.

1. FORMAL STATEMENT OF THE PROBLEM

1.1. Geometry and conventions

We consider the two-body contact problem show on figure 1 where two bodies, (a) and (b), are expected to come into contact during the time interval of interest $[0, \tau]$. To simplify notations, a star $(\star)$ is used to represent indifferently body (a) or (b). Let $\Omega_\star$ be an open bounded subset of the three-dimensional Euclidean space $\mathbb{R}^3$ with a boundary $\partial\Omega_\star$. The set $\Omega_\star$ is occupied by an elastic body $B^\star$. A material point of $B^\star$ is represented by vector co-ordinate $\mathbf{X}^\star = (X_1^\star, X_2^\star, X_3^\star)$ in the undeformed (reference) configuration (doted line in figure 1) while, in the deformed (actual) configuration at time t, this particule is labeled by $\mathbf{x}^\star(\mathbf{X}^\star, t) = (x_1^\star, x_2^\star, x_3^\star)$ (solid line).

The material surface $\partial\Omega_\star$ of each body is decomposed as usual into three mutually disjoint parts $\Gamma_d^\star$, $\Gamma_n^\star$ and $\Gamma_c^\star$. On $\Gamma_d^\star$ (resp. $\Gamma_n^\star$) displacements $\bar{\mathbf{u}}^\star(t)$ (resp. tractions $\mathbf{t}^\star(t)$) are given. We denote by $\Gamma_c^\star$ a portion of body $(\star)$ which is a candidate contact surface. The actual surface on which a body comes into contact with the other one is not known in advance, but is contained in the portion $\Gamma_c^\star$ of $\partial\Omega_\star$. In addition, each body can be subjected to a body force $\mathbf{f}^\star(t)$ (such as gravity for instance).

The displacements of the bodies, relative to the fixed spatial frame, at time t, are represented by a function

$$\mathbf{u} : t \in [0, \tau] \longrightarrow \mathbf{u}(t) = (\mathbf{u}^a(t), \mathbf{u}^b(t)) \in \mathcal{E},$$

where $\mathbf{u}^\star(t)$ is the displacement field[1] of body $(\star)$ at time

[1]The displacement of a material particule P labeled by vector $\mathbf{X}^\star$ is defined as

$$\mathbf{u}^\star(\mathbf{X}^\star, t) = \mathbf{x}^\star(\mathbf{X}^\star, t) - \mathbf{X}^\star.$$

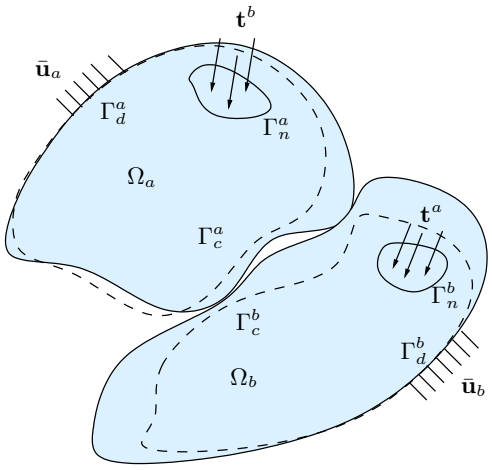

Figure 1: Two elastic bodies (a) and (b) in their undeformed (dash line) and current (solid line) configuration. The actual surface on which the body (a) comes in contact with the other one is not known in advance but is contained in the portion Γ_c^a of its boundary.

t and $\mathcal{E}$ the product of Sobolev spaces of each body

$$\mathcal{E} = (\mathrm{H}^1(\Omega_a))^3 \times (\mathrm{H}^1(\Omega_b))^3.$$

Throughout this study, standard indicial notation and summation convention are employed. Superposed dots $(\dot{})$ indicate differentiation with respect to time and commas $(\ )_{,k}$ denote partial differentiation with respect to x_k. Thus,

$$\dot{u}_i = \frac{\partial u_i}{\partial t}, \quad \ddot{u}_i = \frac{\partial^2 u_i}{\partial t^2}, \quad u_{i,k} = \frac{\partial u_i}{\partial x_k}, \quad \text{etc}$$

1.2. Contact condition

The contact condition on the displacement field $\mathbf{u}$ of a linear elastic body in contact with a frictionless foundation is established by Oden and Kikuchi as

$$\mathbf{u}.\mathbf{n} \leq g_{ap}, \quad \text{on } \Gamma_c, \tag{1}$$

where g_{ap} is a given function representing the normalized gap between the elastic body and the foundation and $\mathbf{n}$ is the outward unit vector normal to the contact surface Γ_c. The extension of this contact condition for Signorini problem to the two-body contact problem has also been achieved. The corresponding impenetrability condition is basically of the same form as the kinematic contact condition (1), except that now the relative displacement field $\mathbf{u}^r = \mathbf{u}^a - \mathbf{u}^b$ is used to give

$$u_n^r \leq g_{ap}, \quad \text{on } \Gamma_c^a, \tag{2}$$

where u_n^r is the normal component of the relative displacement on the contact surface Γ_c^a.

1.3. Hamilton's principle in elastodynamics and variational formulation

Hamilton's principle states that a dynamical system will move so that the time average of the difference, $\mathrm{T}-\mathrm{V}$, between kinetic and total potential energies will be an optimum. In order to be consistent with the static formulation where variational inequalities arise from the minimization of the total potential energy, we seek a minimizer of the Hamilton functional

$$\mathcal{J}(\mathbf{v}) = \int_0^\tau (\mathrm{V} - \mathrm{T})dt, \tag{3}$$

on a constraint set that expresses the impenetrability condition (2). In other word, the objective is to find a displacement $\mathbf{u}$ that minimizes the Hamilton functional $\mathcal{J}$ on a constraint set $\mathcal{K}$. This constraint set depends on the physical problem and its definition plays an important role in the search of the extremum $\mathbf{u}$. For the two-body contact problem, we introduce the space $\mathcal{U}_{ad}$ of admissible displacements $\mathbf{v}$ which verify the Dirichlet boundary conditions defined by

$$\mathcal{U}_{ad} = \{\mathbf{v} \in \mathcal{E} \ \mid \ \mathbf{v}^a = \bar{\mathbf{u}}^a \quad \text{on } \Gamma_d^a, \quad \mathbf{v}^b = \bar{\mathbf{u}}^b \quad \text{on } \Gamma_d^b\}$$

The constraint set $\mathcal{K}$ consists of those displacement fields $\mathbf{v}$ which satisfy the kinematic contact condition (2)

$$\mathcal{K} = \{\mathbf{v} \in \mathcal{U}_{ad} \ \mid \ v_n^r - g_{ap} \leq 0 \quad \text{on } \Gamma_c^a\}$$

where $v_n^r = v_n^a - v_n^b$ is the normal component of the relative displacement on Γ_c^a. This set, $\mathcal{K}$, is not a linear space of $\mathcal{E}$, but a nonempty closed convex subset of $\mathcal{E}$. Thus, using Euler inequality [15], and according to (3), the two-body contact problem has the following variational form

$$\begin{cases} \text{find } \mathbf{u} \in \mathcal{K} \text{ such that, } \forall t \in [0,\tau] \\ m(\ddot{\mathbf{u}}, \mathbf{v}-\mathbf{u}) + k(\mathbf{u}, \mathbf{v}-\mathbf{u}) - f(\mathbf{v}-\mathbf{u}) \geq 0, \quad \forall \mathbf{v} \in \mathcal{K} \end{cases} \tag{4}$$

where the traditional bilinear forms, defined from $\mathcal{E} \times \mathcal{E} \to \mathbb{R}$, for "mass" $m(.,.)$ and "stiffness" $k(.,.)$ respectively,

have been introduced as follow

$$m(\mathbf{u},\mathbf{v}) = \sum_{\star=a,b}\int_{\Omega_\star}\rho_\star u_k^\star v_k^\star\,dv,$$
$$k(\mathbf{u},\mathbf{v}) = \sum_{\star=a,b}\int_{\Omega_\star}C_{klmn}^\star u_{m,n}^\star v_{k,l}^\star\,dv.$$

The symbol $\rho_\star$ denotes the mass density of body $(\star)$ and C_{ijkl} are the components of the Hooke's tensor of elasticity, which possesses the standard symmetries. In formulation (4), $f(.)$ is a linear function on $\mathcal{E}$ representing the virtual work produced by external forces (body forces $\rho_\star\mathbf{f}^\star$ and prescribed tractions $\mathbf{t}^\star$)

$$f(\mathbf{v}) = \sum_{\star=a,b}\left[\int_{\Omega_\star}\rho_\star\mathbf{f}^\star\cdot\mathbf{v}^\star\,dv + \int_{\Gamma_n^\star}\mathbf{t}^\star\cdot\mathbf{v}^\star\,ds\right].$$

1.4. Method of Lagrange multipliers

Constrained minimization problems can be reformulated as saddle point problems using the method of Lagrange multipliers (see Refs. [4] and [15]). Such formulation makes it possible to seek minima of functionals in linear spaces rather than closed convex sets. This is done by introducing, instead of the constraint set $\mathcal{K}$, the space $\mathcal{W}=\mathcal{E}\times\mathcal{Z}\times\mathcal{N}$ where

$$\mathcal{Z} = \mathrm{H}^{-1/2}(\Gamma_d^a)\times\mathrm{H}^{-1/2}(\Gamma_d^b) \tag{5}$$

is the dual space of displacements on the Dirichlet surfaces while $\mathcal{N}$ is the admissible set for the Lagrange multipliers p_n defined by

$$\mathcal{N} = \{p_n\in\mathrm{H}^{-1/2}(\Gamma_c)\ \mid\ p_n\le 0\quad\text{on }\Gamma_c^a\}. \tag{6}$$

The set $\mathcal{N}$ is a subset of the dual space of displacements on Γ_c containing negative force. The minimization problem (4) is then equivalent to the determination of the saddle point $(\mathbf{u},\boldsymbol{\chi},\sigma_n)\in\mathcal{W}$ of the Lagrangian $\mathcal{L}(\mathbf{v},\boldsymbol{\kappa},p_n)\in\mathbb{R}$ defined by

$$\mathcal{L} = \mathcal{J}(\mathbf{v}) - \int_0^\tau\left[\sum_{\star=a,b}(\boldsymbol{\kappa}^\star|\mathbf{v}^\star-\bar{\mathbf{u}}^\star)_{\Gamma_d^\star} + (p_n|v_n^r-g_{ap})_{\Gamma_c}\right]dt$$

where $(\,.\,|\,.\,)_{\Gamma_d^\star}$ and $(\,.\,|\,.\,)_{\Gamma_c}$ are the duality pairing on $\mathrm{H}^{-1/2}(\Gamma_d^\star)\times\mathrm{H}^{1/2}(\Gamma_d^\star)$ and $\mathrm{H}^{-1/2}(\Gamma_c^a)\times\mathrm{H}^{1/2}(\Gamma_c^a)$ respectively. This saddle point satisfies the following equations and inequation

Find $(\mathbf{u},\boldsymbol{\chi},\sigma_n)\in\mathcal{W}$ such that

$$m(\ddot{\mathbf{u}},\mathbf{v})+k(\mathbf{u},\mathbf{v}) = b(\mathbf{v}) \qquad \forall\mathbf{v}\in\mathcal{E} \tag{7a}$$
$$\sum_{\star=a,b}(\boldsymbol{\kappa}^\star|\mathbf{u}^\star-\bar{\mathbf{u}}^\star)_{\Gamma_d^\star} = 0 \qquad \forall\boldsymbol{\kappa}\in\mathcal{Z} \tag{7b}$$
$$(p_n-\sigma_n|u_n^r-g_{ap})_{\Gamma_c^a}\ge 0 \qquad \forall p_n\in\mathcal{N} \tag{7c}$$

where $b(\mathbf{v})$ represents the forces acting on solids (a) and (b)

$$b(\mathbf{v}) = f(\mathbf{v}) + \sum_{\star=a,b}(\boldsymbol{\chi}^\star|\mathbf{v}^\star)_{\Gamma_d^\star} + (\sigma_n|v_n^r)_{\Gamma_c^a}, \quad \forall\mathbf{v}\in\mathcal{E}. \tag{8}$$

The first equation (7a) represents the principle of virtual work (power) applied to the bodies (a) and (b) subjected, on one hand, to external forces $f(\mathbf{v})$ and to reaction forces $\boldsymbol{\chi}^\star$ on their respective Dirichlet surface $\Gamma_d^\star$, and on the other hand, to a contact pressure σ_n normal to the contact surface Γ_c^a. Note the sign reversal in the contact pressure in (8) according to Newton's third law,

$$(\sigma_n|v_n^r)_{\Gamma_c^a} = (\sigma_n|v_n^a)_{\Gamma_c^a} - \left(\sigma_n|v_n^b\right)_{\Gamma_c^b}$$

($\mathbf{n}$ is the outward unit vector normal to Γ_c^a). The second equation (7b) expresses the Dirichlet boundary conditions. Finally, the variational inequality (7c) expresses the unilateral and frictionless contact condition on $\Gamma_c^\star$.

1.5. Equation of motion

Using the Green formula, the classical strong form of the two-body contact problem can also be obtained from the formulation (7)

$$\rho_\star\ddot{u}_k^\star = \sigma_{kl,l}^\star + \rho_\star f_k^\star \qquad \text{in }\Omega_\star\times[0,\tau] \tag{9a}$$
$$\sigma_{kl}^\star n_l^\star = t_k^\star \qquad \text{on }\Gamma_n^\star\times[0,\tau] \tag{9b}$$
$$\left.\begin{array}{l}\sigma_{kl}^\star n_l^\star = \chi_k^\star\\ u_k^\star = \bar{u}_k^\star\end{array}\right\} \qquad \text{on }\Gamma_d^\star\times[0,\tau] \tag{9c}$$
$$\left.\begin{array}{l}u_n^r - g_{ap}\le 0\\ \sigma_n\le 0,\quad \boldsymbol{\sigma}_{T_k}^\star = 0\\ \sigma_n(u_n^r-g_{ap}) = 0\\ \sigma_n = \sigma_{kl}^\star n_l^\star n_k^\star\\ u_n^r = u_n^a - u_n^b\end{array}\right\} \qquad \text{on }\Gamma_c\times[0,\tau] \tag{9d}$$

This step is not a straightforward exercise. In fact, it can be shown that any sufficiently smooth solution of (4) or (7) is also a solution of (9). Conversely, taking $\mathbf{u}$ and $\mathbf{v}$ in the convex set $\mathcal{K}$, multiplying (9a) by $v_k^\star-u_k^\star$ and integrating by parts over $\Omega_\star$, it is possible to obtain the variational inequality (4) and consequently (7). The relationship between the solution of the variational inequality (4) (or, equivalently (7)) and the solution of the classical problem (9) can be found in Ref. [4]. More precisely, these relationships are established by Kikuchi and Oden [4] only in the static context where inertial effects are not taking into account.

To our knowledge, the question of existence and especially of uniqueness for the frictionless dynamic contact problems stated above is still open. Uniqueness of solution, in the dynamic context, is only proved by Duvaut and Lions [6] for frictional contacts assuming prescribed normal tractions. Their demonstration, based on energy considerations, can not be applied in our case where the normal unilateral traction is an unknown.

In fact, the two body contact problem is not yet well-posed since several solutions can be obtained from the variational statement (4) or, equivalently (7). Appendix A.1 is an illustration of such a case.

2. DYNAMICAL CONTACT CONDITION

2.1. Energy dissipation during contact

As it is illustrated in appendix (A.1), any physically relevant solution of the contact problem has to be found by explicitely adressing the energy equation. How the energy is dissipated in the two-body contact problem ? To answer to this question, let us compute the total time rate of change in energy (kinetic T and internal W) by replacing the virtual velocity $\mathbf{v} \in \mathcal{E}$ by the real velocity $\dot{\mathbf{u}}$ in (7a) to obtain

$$\frac{dE}{dt} = \frac{d(T+W)}{dt} = b(\dot{\mathbf{u}})$$

where the linear form $b(\mathbf{v})$ is given by (8). This variation of energy, according to the first principle of thermodynamics, balances the total supply of energy per unit time through external forces and heat: $\mathcal{P} + \mathcal{Q}$. According to (8), it is clear that the rate of work of all external forces is

$$\mathcal{P} = f(\dot{\mathbf{u}}) + \sum_{\star=a,b} (\boldsymbol{\chi}^\star | \dot{\mathbf{u}}^\star)_{\Gamma_d^\star} .$$

Thus, the heat energy that enters into the body per unit time, i.e. the heat rate, is given by

$$\mathcal{Q} = (\sigma_n | \dot{u}_n^r)_{\Gamma_c^a}$$

where $\dot{u}_n^r = \dot{u}_n^a - \dot{u}_n^b$ is the normal component of the relative velocity on Γ_c^a. In order to obtain a well-posed problem a new contact condition must be found specifying the value of this dissipation term. This the purpose of section 2. This condition is called the *dynamical contact condition* as it is not necessary for static problems.

2.2. Balance laws on the contact surface

The dynamical contact condition will be found by adjusting the balance laws[2] of physical quantities on the contact surface to the impenetrability condition (see Refs. [16, 17, 18, 19] and the thesis [20]). This condition, used in inequality (2), can be also formulated by

> *Two bodies do not penetrate if the flux of mass through their separation surface Γ_c (see figure 2), of velocity $\mathbf{w}$, vanishes, i.e,*
>
> $$\rho_\star(\dot{u^\star}_k - w_k)n_k = 0 \quad on\ \Gamma_c \qquad (10)$$
>
> *where $\rho_\star$ is the mass density of body $(\star)$ and $\mathbf{n}$ the unit vector normal to Γ_c outgoing from body (a).*

[2]Conservation of mass, momentum, moment of momentum, energy and second thermodynamic law.

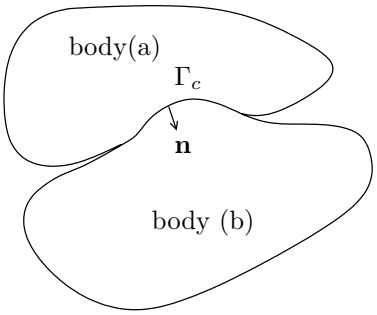

Figure 2: The surface Γ_c is called contact surface or sliding surface.

According to this hypothesis, the balance laws [3] of physical quantities give rise to the following properties on Γ_c

$$[\![\dot{u}_k]\!]_{\Gamma_c} n_k = \dot{u}_n^b - \dot{u}_n^a = -\dot{u}_n^r = 0 \quad \text{mass conservation} \qquad (11)$$

$$[\![\sigma_{kl}]\!]_{\Gamma_c} n_l = 0 \quad \text{momentum conservation} \qquad (12)$$

$$[\![\sigma_{kl}.\dot{u}_k]\!]_{\Gamma_c} n_l = [\![q_l]\!]_{\Gamma_c} n_l \quad \text{energy conservation} \qquad (13)$$

$$[\![q_l]\!]_{\Gamma_c} n_l \geq 0 \quad \text{2nd thermodynamic law} \qquad (14)$$

where $\boldsymbol{\sigma}$ is the Cauchy stress tensor and $\mathbf{q}$ the heat flux vector. The jump $[\![.]\!]_{\Gamma_c}$ is a spatial jump through the contact surface: these brackets indicate the difference of their enclosure at the surface Γ_c approached from the positive and negative sides of its positive normal, e.g., $[\![f]\!] \equiv f^+ - f^-$ and thus the product $[\![f]\!]\, n_k$ is independent of the normal's orientation or coordinate system.

According to (11), the velocity $\dot{\mathbf{u}}$ undergoes a discontinuity through Γ_c, but this discontinuity is purely tangential. Equation (12) stipulates that the stress vector is continuous through Γ_c. Decomposing the stress vector and the velocity into their normal and tangential components

$$\begin{aligned} \sigma_{kl} n_l &= \sigma_n n_k + \sigma_{T_k} \\ [\![\dot{u}_k]\!]_{\Gamma_c} &= ([\![\dot{u}_i]\!]_{\Gamma_c} n_i) n_k + [\![\dot{u}_{T_k}]\!]_{\Gamma_c} , \end{aligned}$$

the conservation of energy through the contact surface (13) yields, according to (12)

$$\sigma_n\, [\![\dot{u}_k]\!]_{\Gamma_c} n_k + \sigma_{T_k}\, [\![\dot{u}_{T_k}]\!]_{\Gamma_c} = [\![q_l]\!]_{\Gamma_c} n_l \geq 0 \quad \text{on } \Gamma_c \qquad (15)$$

Taking into account the conservation of mass (11), this leads to the tangential contact condition

$$\sigma_{T_k}\, [\![\dot{u}_{T_k}]\!]_{\Gamma_c} = [\![q_l]\!]_{\Gamma_c} n_l \geq 0 \quad \text{on } \Gamma_c$$

[3]These balance laws refer to the current (deformed) configuration of the bodies (Eulerian configuration). For contact problems, the boundaries of the bodies are unknown at the outset and must be determined from the solution of differential equations. It is then convenient to employ a formulation based on the reference (undeformed) configuration where the boundary conditions are known (Lagrangian configuration). This provides a reasonable amount of simplicity in dealing with contact problems even though the field equations may be more complicated. Fortunately, within the infinitesimal deformation theory there will be no distinctions among Lagrangian and Eulerian forms of balance laws and jump conditions (see Ref. [16]).

and to the normal contact condition

$$\sigma_n \left[\!\left[\dot{u}_k\right]\!\right]_{\Gamma_c} n_k = 0, \quad \text{on } \Gamma_c$$

or, equivalently (since Γ_c can be replaced by Γ_c^a in the linear theory)

$$(\sigma_n | \dot{u}_n^r)_{\Gamma_c^a} = 0 \tag{16}$$

These conditions indicate that only tangential tractions can generate energy dissipation by friction between particles on the contact surface. In this article only frictionless contact problems are considered so $\sigma_T = 0$ on Γ_c, but the contact condition (16) is still valid even if the contact is considered with friction.

According to the contact condition (16) a non-zero traction may only be generated if the normal velocity $\dot{u}_n$ is continuous through the contact surface. In other words, during interaction the normal velocities of both bodies must be equal on the contact area, which is quite intuitive. This condition (16) is sometimes called the persistency condition and it is of particular importance in the design of numerical algorithms for dynamic contact problems (see Laursen et *al* [21, 11, 22] and Taylor et *al* [10]).

In fact, the impact between portions of the boundaries of elastic bodies is expected to produce propagating stress and velocity discontinuities. Indeed, just before contact, the relative normal velocity $\dot{u}_n^r$ could be non-zero: this velocity must thus make a jump to vanish during contact. That is to say that at least one of the bodies endures a brutal change in its velocity in the direction normal to Γ_c. Thus, a particular attention must be dedicated to this additional difficulty.

In conclusion to this section: the contact problem is now well posed by added contact condition (16) to the variational constrained problem (7).

3. RECIPROCAL FORMULATION

To compute a solution of the two-body contact problem in case of stress and velocity discontinuities we will prefer to use an integral representation with Green functions rather than finite difference algorithms such as Newmark and central difference schemes. This method is usually called reciprocal formulation as it involves the inverse of the *elasticity operator* appearing in standard variational statements of linear elastodynamic problems. This inverse operator is the Green function. One of the advantage of this method is that the awkward problem of discontinuities, mentioned just above, is already treated in the definition of the Green function without the complications of contact problems. Moreover, since the contact pressure occurs only on the contact surface Γ_c the reciprocal formulation uses functions defined only on this surface. It is then often possible to approximate the system using considerably fewer unknowns than with classical formulations and then save computational time.

To deal with integral representation using Green functions, it is convenient to first investigate the unconstrained problem by considering one of the two bodies. This is the purpose of the next subsection where the mathematical tools needed for the reciprocal formulation will be defined. A semi-analytical method will also be described to compute those tools. In the following subsection 3.2, the reciprocal formulation will be applied to the two-body contact problem and this will lead to a very simple numerical algorithm described in subsection 3.3 and 3.4.

3.1. The unconstrained problem

3.1.1. Green and Poisson functions

For the time being, let us consider one of the two bodies, say body ($\star$) for example, and suppose that the contact pressure σ_n is a given prescribed traction on a $\Gamma_c^\star$. If the sources $\rho_\star \mathbf{f}^\star$, $\mathbf{t}^\star$ and the Dirichlet boundary condition $\bar{\mathbf{u}}^\star$ on $\Gamma_d^\star$ are also prescribed, the displacement field $\mathbf{u}^\star$, solution of the variational formulation (7a-7b) (written for one solid) is unique and can be expressed by an integral representation (see Refs. [23, 24]) using Green and Poisson functions, namely

$$\begin{aligned} u_k^\star(\mathbf{x};t) &= < \mathbf{G}^k | \rho_\star \mathbf{f}^\star >_{\Omega^\star} + < \mathbf{N}^k | \mathbf{t}^\star >_{\Gamma_n^\star} \\ &+ < \mathbf{N}^k | \sigma_n \mathbf{n}^\star >_{\Gamma_c^\star} + < \mathbf{D}^k | \bar{\mathbf{u}}^\star >_{\Gamma_d^\star} \end{aligned} \tag{17}$$

where the notation $< .|. >_A$ expresses the spatio-temporal convolution

$$< \mathbf{O}^k | \boldsymbol{\phi} >_A = \int_0^t \int_A O_i^k(\mathbf{x}, \mathbf{y}; t-\tau) \phi_i^\star(\mathbf{y};\tau) dA_{\mathbf{y}} d\tau$$

whenever A is a surface or a volume in $\mathbb{R}^3$. In the formula (17), the Green function $\mathbf{G}^k(\mathbf{x}, \mathbf{y}; t)$ is the solution of the variational unconstrained problem (7a-7b) with vanished sources, excepted

$$\rho_\star \mathbf{f}^\star = \delta(t)\delta(\mathbf{x}-\mathbf{y})\mathbf{e}_k, \quad \mathbf{x} \in \bar{\Omega}^\star, \quad \mathbf{y} \in \Omega^\star$$

where $\mathbf{e}_k$ is k-th unit basis vector of $\mathbb{R}^3$. The Poisson functions $\mathbf{N}^k$ and $\mathbf{D}^k$ are the displacement fields corresponding to an impulsive source (force and displacement respectively) placed on the surface of the body. This yields, on the Neumann's surface Γ_n, to the Poisson function[4] $N^k(\mathbf{x}, \mathbf{y}; t)$ with the source

$$\mathbf{t}^\star = \delta(t)\delta(\mathbf{x}-\mathbf{y})\mathbf{e}_k, \quad \mathbf{x} \in \bar{\Omega}^\star, \quad \mathbf{y} \in \Gamma_n^\star$$

and, on the Dirichlet's surface, to the Poisson function $D^k(\mathbf{x}, \mathbf{y}; t)$ with the source

$$\bar{\mathbf{u}}^\star = \delta(t)\delta(\mathbf{x}-\mathbf{y})\mathbf{e}_k, \quad \mathbf{x} \in \bar{\Omega}^\star, \quad \mathbf{y} \in \Gamma_d^\star$$

It is important to note that the integral representation (17) has the same form for a point $\mathbf{x}$ in the domain $\Omega^\star$ or on the boundary $\partial\Omega^\star = \Gamma_n^\star \cup \Gamma_d^\star$. This is an alternative to the integral representation that uses the fundamental solution (free-space Green's function). In this case, a different expression exists depending on the position of the point field $\mathbf{x}$ (see Ref. [25]).

[4] Same procedure can be done for the contact surface Γ_c.

3.1.2. Modal theory

The major problem of reciprocal method is to find the Green and Poisson functions related to an elastic body. In practice only a few physical systems allow an analytical calculation of such functions. Discontinuities in the fields make difficult to compute pure numerical solutions of the unconstrained variational problem with impulse sources. Modal theory[5] gives an opportunity to compute semi-analytical function: the Green function $\mathbf{G}^k$ (and even the Poisson $\mathbf{N}^k$) for any point $\mathbf{x}$ and time t may be represented by a normal-mode expansion

$$\mathbf{G}^k(\mathbf{x},\mathbf{y};t) = \sum_{n=1}^{\infty} \boldsymbol{\phi}_n^\star(\mathbf{x}) a_n(\mathbf{y};t) \tag{18}$$

where $\boldsymbol{\phi}_n^\star$ is the n-th mode of the body $(\star)$ satisfying homogeneous boundary conditions. Substitution of the series representation into the variational formulation (7a-7b) with the convenient choice of $\mathbf{v} = \boldsymbol{\phi}_m^\star$ gives an ordinary differential equation which can be solved analytically by Laplace transform method. This yields to the Green function, valid for $(\mathbf{x},\mathbf{y}) \in \bar{\Omega}^\star \times \Omega^\star$,

$$\mathbf{G}^k(\mathbf{x},\mathbf{y};t) = \sum_{n=1}^{\infty} \boldsymbol{\phi}_n^\star(\mathbf{x}) Y(t) \frac{\sin \omega_n t}{m_n \omega_n} \boldsymbol{\phi}_n^\star(\mathbf{y}) \cdot \mathbf{e}_k, \tag{19}$$

where m_n and ω_n are respectively the modal mass and modal angular frequency associated to the n-th mode respectively and $Y(t)$ is the Heaviside function. A similar expression can be built for the Poisson function where the point $\mathbf{y}$ lie on the Neumann surface[6]: $(\mathbf{x},\mathbf{y}) \in \bar{\Omega}^\star \times \Gamma_n^\star$,

$$\mathbf{N}^k(\mathbf{x},\mathbf{y};t) = \sum_{n=1}^{\infty} \boldsymbol{\phi}_n^\star(\mathbf{x}) Y(t) \frac{\sin \omega_n t}{m_n \omega_n} \boldsymbol{\phi}_n^\star(\mathbf{y}) \cdot \mathbf{e}_k, \tag{20}$$

Those formulae are also valid for rigid body modes where the eigen frequency vanish, since $\lim_{\omega_n \to 0} \frac{\sin \omega_n t}{m_n \omega_n} = \frac{t}{m_n}$. The Poisson function $\mathbf{D}^k$ can also be computed using normal-mode expansion. But, since the modes vanish on the Dirichlet surface $\Gamma_d^\star$, a more complicated approach must be used (see Ref. [26] for details).

3.2. Two-body contact problem

Applying this result to the variational constrained problem (7), the displacement and the velocity on the contact surface can be expressed as functions of the contact pressure. The two-body contact problem is then reduced to the impenetrability (7c) and to the dynamical contact condition (16) with only one unknown: the contact pressure.

find $\sigma_n \in \mathcal{N}$, such that

$$(p_n - \sigma_n | G_d(\sigma_n) + \widetilde{g_{ap}})_{\Gamma_c} \geq 0, \qquad \forall p_n \in \mathcal{N} \tag{21a}$$

and

$$\left(\sigma_n | G_v(\sigma_n) + \widetilde{\dot{u}}_n^r\right)_{\Gamma_c} = 0 \tag{21b}$$

where G_d and G_v

$$\begin{aligned} G_d(\sigma_n) &= \int_{\Gamma_c} N(\mathbf{x},\mathbf{y};t) * \sigma_n(\mathbf{y};t)\, ds_{\mathbf{y}} \\ G_v(\sigma_n) &= \int_{\Gamma_c} \dot{N}(\mathbf{x},\mathbf{y};t) * \sigma_n(\mathbf{y};t)\, ds_{\mathbf{y}} \\ \widetilde{g_{ap}} &= \widetilde{u}_n^r - g_{ap}. \end{aligned}$$

Let us see how this substitution is made. The normal displacement on the contact surface $\Gamma_c^\star$ of the body $(\star)$, $u_n^\star(\mathbf{x};t) = u_k^\star(\mathbf{x};t) n_k(\mathbf{x})$, have been decomposed as contact and external contributions

$$u_n^\star(\mathbf{x};t) = u_{\text{cont.}}^\star(\mathbf{x};t) + \widetilde{u}_n^\star(\mathbf{x};t), \quad \mathbf{x} \in \Gamma_c^\star.$$

In this way, the part of the displacement due to the contact pressure is

$$u_{\text{cont.}}^\star(\mathbf{x};t) = \int_{\Gamma_c^\star} N_n^\star(\mathbf{x},\mathbf{y};t) * \sigma_n(\mathbf{y};t)\, ds_{\mathbf{y}} \tag{22}$$

where here, the Poisson function

$$N_n^\star(\mathbf{x},\mathbf{y};t) = n_i(\mathbf{y}) N_i^k(\mathbf{x},\mathbf{y};t) n_k(\mathbf{x}), \quad \mathbf{x},\mathbf{y} \in \Gamma_c$$

represents the normal displacement at point $\mathbf{x} \in \Gamma_c^\star$ resulting from an impulse force applied, at time $t = 0$, at point $\mathbf{y} \in \Gamma_c^\star$ in the direction normal to $\Gamma_c^\star$.

The displacement, $\widetilde{u}_n^\star$, is a known function for a given set of external contributions $\rho_\star \mathbf{f}^\star$, $\mathbf{t}^\star$ and $\bar{\mathbf{u}}^\star$ and can be expressed, using (17), by the integral representation (normal projection)

$$\begin{aligned} \widetilde{u}_n^\star(\mathbf{x};t) &= < \mathbf{G}^k n_k | \rho_\star \mathbf{f}^\star >_{\Omega^\star} + < \mathbf{N}^k n_k | \mathbf{t}^\star >_{\Gamma_n^\star} \\ &\quad + < \mathbf{D}^k n_k | \bar{\mathbf{u}}^\star >_{\Gamma_d^\star} \end{aligned}$$

In the same manner, normal velocity can be decomposed as contact and external contributions as follows

$$\dot{u}_n^\star(\mathbf{x};t) = \int_{\Gamma_c^\star} \dot{N}_n^\star(\mathbf{x},\mathbf{y};t) * \sigma_n(\mathbf{y};t)\, ds_{\mathbf{y}} + \widetilde{\dot{u}}_n^\star(\mathbf{x};t) \tag{23}$$

where now, $\dot{N}_n^\star$ is the Poisson velocity function of body $(\star)$ which represents the normal velocity at point $\mathbf{x} \in \Gamma_c^\star$ resulting from the same excitation force as for the Poisson function. So, the relative normal displacement, $u_n^r(\mathbf{x};t) = u_n^a - u_n^b$, and velocity, $\dot{u}_n^r(\mathbf{x};t) = \dot{u}_n^a - \dot{u}_n^b$ are functions of the contact pressure

$$\begin{aligned} u_n^r(\mathbf{x};t) &= \widetilde{u}_n^r(\mathbf{x};t) \\ &\quad + \int_{\Gamma_c} N(\mathbf{x},\mathbf{y};t) * \sigma_n(\mathbf{y};t)\, ds_{\mathbf{y}} \qquad (24) \\ \dot{u}_n^r(\mathbf{x};t) &= \widetilde{\dot{u}}_n^r(\mathbf{x};t) \\ &\quad + \int_{\Gamma_c} \dot{N}(\mathbf{x},\mathbf{y};t) * \sigma_n(\mathbf{y};t)\, ds_{\mathbf{y}} \qquad (25) \end{aligned}$$

[5] Althought Green functions are computed, in this article, by modal theory please note that other methods exist to obtain those kernels (finite difference algorithms, integral formalism ...).

[6] instead of being in the domain $\Omega_\star$

where $N(\mathbf{x},\mathbf{y};t) = N_n^a(\mathbf{x},\mathbf{y};t) + N_n^b(\mathbf{x},\mathbf{y};t)$ represents the relative Poisson function defined for $\mathbf{y}$ on the contact surface (the plus sign (+) is due to opposite normal unit vectors $\mathbf{n}^a$ and $\mathbf{n}^b$). Finaly, these integral representations (24) and (25) have been replaced into the contact condition (7c) and (16) respectively to give the reciprocal variational problem (21).

For static problems, the dynamic contact condition (21b) does not exist and the reciprocal variational problem can be alternatively formulated as a constrained minimization problem, on the convex set $\mathcal{N}$, of the functional

$$F(p_n) = \frac{1}{2}\,(p_n|G_0(p_n))_{\Gamma_c} + (p_n|\widetilde{g_{ap}})_{\Gamma_c}$$

where $G_0(p_n) = \int_{\Gamma_c} N(\mathbf{x},\mathbf{y})p_n(\mathbf{y})\,ds_{\mathbf{y}}$ and $N(\mathbf{x},\mathbf{y})$ is a time-independent Poisson function. An iterative scheme to obtain a solution of such a problem, using a variant of Uzawa's method, can be found in [4] and in [20]. These procedure can accelerate convergence during an iteration of the scheme which deals with a set of candidate contact nodes (or surfaces). The dynamic problems are not so straightforward and the reciprocal formulation can be simplified using a time discretization that transforms convolutions into discrete sums.

3.3. Time discretization and algorithm

A time discretization of the two-body contact problem is obtained by introducing a partition of the time domain $[0,\tau]$ in consideration in M intervals of length Δt such that $0 = t_0 < t_1 < \ldots < t_M = \tau$, with $t_{k+1} - t_k = \Delta t$. In addition, the contact pressure σ_n is postulated, in this model, to be a succession of impulse forces such that

$$\sigma_n(\mathbf{x},t) \simeq \sum_{k=0}^{M} \sigma_n(\mathbf{x},t_k)\delta(t-t_k) \equiv \sum_{k=0}^{M} \sigma_n(\mathbf{x},k)\delta_k.$$

Thus the convolution that appears in formula (24) can be replaced by the discrete sum

$$N(\mathbf{x},\mathbf{y};t) * \sigma_n(\mathbf{y};t) \simeq \sum_{l=0}^{k} N(\mathbf{x},\mathbf{y};k-l)\sigma_n(\mathbf{y},l)$$

and then can be split, with respect to the contact pressure, into instantaneous[7] and historical terms

$$\simeq N(\mathbf{x},\mathbf{y};0^+)\sigma_n(\mathbf{y},k) + \sum_{l=0}^{k-1} N(\mathbf{x},\mathbf{y};k-l)\sigma_n(\mathbf{y},l).$$

Thus, the normalized distance between body (a) and (b), at time t_k, which should exist in absence of contact, can be evaluated by

$$\widehat{u}_n^r(\mathbf{x};k) = \widetilde{u}_n^r(\mathbf{x};k) + \int_{\Gamma_c} \sum_{l=0}^{k-1} N(\mathbf{x},\mathbf{y};k-l)\sigma_n(\mathbf{y},l)\,ds_{\mathbf{y}}. \tag{26}$$

[7] Here $N(\mathbf{x},\mathbf{y};0^+)$ is in fact the jump $N(\mathbf{x},\mathbf{y};0^+) - N(\mathbf{x},\mathbf{y};0^-)$, but $N(\mathbf{x},\mathbf{y};0^-)$ is zero by causality.

This relative distance can be greater than the normalized gap function on a portion $\Gamma_c(k)$ of the candidate contact surface Γ_c (see the contact condition (2)). If this surface is not empty, a contact occurs between the time t_{k-1} and t_k producing a pressure to avoid the penetration of the bodies. In order to obtain a very simple algorithm, the contact pressure is postulated to act at discrete time t_k (and not between t_{k-1} and t_k). In other word a small penetration[8] is tolerated. On the extended contact area $\Gamma_c(k)$, which varies on time, the particles velocities can be computed in the same way

$$\dot{u}_n^r(\mathbf{x};k) = \widehat{\dot{u}}_n^r(\mathbf{x};k) + \int_{\Gamma_c(k)} \dot{N}(\mathbf{x},\mathbf{y};0^+)\sigma_n(\mathbf{y};k)\,ds_{\mathbf{y}} \tag{27}$$

where the velocity

$$\widehat{\dot{u}}_n^r(\mathbf{x};k) = \widetilde{\dot{u}}_n^r(\mathbf{x};k) + \int_{\Gamma_c} \sum_{l=0}^{k-1} \dot{N}(\mathbf{x},\mathbf{y};k-l)\sigma_n(\mathbf{y},l)\,ds_{\mathbf{y}} \tag{28}$$

is a known function consisting of external and historical contributions and does not depend on the contact pressure at time t_k. Finally, according to the dynamical contact condition (16), equation (27) must vanish in order to create non-zero tractions and give the opportunity to calculate the contact pressure at time t_k by the integral equation

$$\int_{\Gamma_c(k)} \dot{N}(\mathbf{x},\mathbf{y};0^+)\sigma_n(\mathbf{y};k)\,ds_{\mathbf{y}} = -\widehat{\dot{u}}_n^r(\mathbf{x};k). \tag{29}$$

The contact algorithm can be summarized as:

$$\left\{\begin{array}{ll}
\text{initialize } \sigma_n \text{ to 0 for all } k \in [1,\text{sample-length}] & \\
\text{for } k = 1 \ldots \text{sample-length} & \\
\quad \text{compute } \widehat{u}_n^r(k) & \text{by Eq. (26)} \\
\quad \text{if } \widehat{u}_n^r(k) > G_{ap} \text{ then} & \\
\quad\quad \text{compute } \widehat{\dot{u}}_n^r(k) & \text{by Eq. (28)} \\
\quad\quad \text{compute } \sigma_n(k) \text{ for positive relative velocity} & \text{by Eq. (29)} \\
\quad \text{end} & \\
\quad k = k+1 & \\
\text{end} &
\end{array}\right. \tag{30}$$

Note that the relative velocity $\widehat{\dot{u}}_n^r(k)$ is positive when a contact occurs between the bodies. But, since a small penetration is tolerated, a negative velocity could be computed and a positive contact pressure would be produced. To avoid such an error a test is done.

3.4. Approximation and numerical analysis

A finite element approximation of the variational unconstrained problem (7a-7b) is now considered in order

[8] This small penetration is not a restriction in the model: by calculating the exact moment of contact, an algorithm without any penetration can be built. This procedure slows down calculation without making real improvement and it is not chossen for ours applications.

to compute the Green and Poisson functions. Each domain $\bar{\Omega}^\star$ is partitioned into a mesh of finite elements $\bar{\Omega}_h^\star$ over which piecewise polynomial approximations of the displacement field $\mathbf{u}$ at each time are introduced. This process can lead to the construction of a family $\{\mathcal{E}_h^\star\}$ of finite-dimensional subspaces of each Sobolev space $\mathcal{E}^\star = (\mathrm{H}^1(\Omega_\star))^3$. Here h is an appropriate mesh parameter (typically h is the diameter of the largest element in the finite element mesh). The vector $\mathbf{u}_h^\star$ of $\mathcal{E}_h^\star$, finite-dimensional counterpart of the displacement vector $\mathbf{u}^\star$, can be expressed as

$$\mathbf{u}_h^\star(\mathbf{x},t) = \sum_{\alpha=1}^{N_h^\star} \mathbf{U}_\star^\alpha(t)\psi_\alpha^\star(\mathbf{x}), \quad \mathbf{x} \in \bar{\Omega}_h^\star \quad \star = \text{a or b} \quad (31)$$

where $\psi_\alpha^\star$ denote basis functions spanning $\mathcal{E}_h^\star$, and $N_h^\star$ is the total number of node of the finite element mesh $\bar{\Omega}_h^\star$. Since[9] $\psi_\alpha^\star(\mathbf{x}^\beta) = \delta_\alpha^\beta$ at a node $\mathbf{x}^\beta \in \bar{\Omega}_h^\star$, $\mathbf{U}_\star^\alpha(t) = \mathbf{u}_h^\star(\mathbf{x}^\alpha, t)$ holds. If the summation convention is extended to the case $a^\alpha b_\alpha = \sum_{\alpha=1}^{N_h} a^\alpha b_\alpha$, the time derivatives of $\mathbf{u}_h^\star$ are

$$\dot{\mathbf{u}}_h^\star(\mathbf{x},t) = \dot{\mathbf{U}}_\star^\alpha(t)\psi_\alpha^\star(\mathbf{x}), \quad \ddot{\mathbf{u}}_h^\star(\mathbf{x},t) = \ddot{\mathbf{U}}_\star^\alpha(t)\psi_\alpha^\star(\mathbf{x})$$

The finite element method applied to the variational problem (7a-7b) makes it possible to compute, for each discrete time t_k and for each body $(\star)$, a matrix $\mathbb{N}^\star(k)$ using normal-mode expansion (20). This matrix is an approximation of the Poisson functions $N^\star(\mathbf{x},\mathbf{y};t)$ of size $(M_c \times M_c)$ where M_c is the total number of nodal points on the candidate contact surface Γ_c. The matrix components $\mathbb{N}_{ij}^\star(.)$ is a discrete time function representing the displacement at node i due to an impulse force applied on node j.

At the third step of the contact algorithm (30), the relative Poisson function $\mathbb{N} = \mathbb{N}^a + \mathbb{N}^b$ is used to compute the normal displacement, at time t_k, which should exist in absence of contact

$$\widehat{\mathbf{U}}_n^r(k) = \widetilde{\mathbf{U}}_n^r(k) + \sum_{l=0}^{k-1} \mathbb{N}(k-l)\mathbf{P}_n(l) \quad (32)$$

where $\mathbf{P}_n$ represents the numerical approximation of the unknown contact pressure σ_n. In case of contact, the relative velocity

$$\widehat{\dot{\mathbf{U}}}_n^{\,r}(k) = \widetilde{\dot{\mathbf{U}}}_n^{\,r}(k) + \sum_{l=0}^{k-1} \dot{\mathbb{N}}(k-l)\mathbf{P}_n(l) \quad (33)$$

is computed using a similar matrix $\dot{\mathbb{N}} = \dot{\mathbb{N}}^a + \dot{\mathbb{N}}^b$. This velocity is evaluated only on the time dependent surface $\Gamma_c(k)$ which is represented by a set Λ_k of nodal points in contact at time t_k. Finally, to solve the integral equation (29), the relative velocity Poisson matrix $\dot{\mathbb{N}}$ is evaluated for $k = 0$, and leads, for each time t_k, to the linear system

$$\dot{\mathbb{N}}^{\Lambda_k}\mathbf{P}_n(k) = -\widehat{\dot{\mathbf{U}}}_n^{\,r}(k) \quad (34)$$

where $\dot{\mathbb{N}}^{\Lambda_k}$ is the restriction of the matrix $\dot{\mathbb{N}}(0^+)$ to the set Λ_k. The solution $\mathbf{P}_n(k)$ of this linear system will give the possibility to continue the contact algorithm for time $k = k+1$.

3.5. Numerical performance of the algorithm

The performance of the proposed algorithm is related to the fact that the overall computation cost can be split in two phases:

1. computation of the kernels (Green and Poissons functions) to express a integral solution as a function of the contact force
2. real-time iterative procedure to obtain this force to predict by convolution the evolution of the system.

Since a integral solution is proposed, the reader is invited to consider the fact that no differential equation has to be solved and thus finite difference methods are not eligibled. Futhermore no integral equation has also to be solved in a sense of the boundary element method.

Once Green and Poisson functions have been computed and stored, as can be seen in the pseudo code (30), the computation cost is mostly due to the determination of the contact force σ_n since the convolution cost, used to computed displacements and velocities, can be negleted. At each time step, a linear system (34) has to be solved. An examination of the admittance matrix's properties, $\dot{\mathbb{N}}(0^+)$, reveals that this system is almost diagonal since the matrix quantifies the information propagation between nodes on the contact surface (here lies the major difference between the present method and boundary element methods, where the matrices are dense).

In theory, the continuous admittance operator is perfectly diagonal, since the speed of sound is finite. This property guarantees the convergence of the iterative solution of the nonlinear equations. But, the influence of the numerical approximation of such an operator on the convergence criterion is still needed an will be a perspective of this work. In practice, the iterative scheme converges in few iterations.

The slowness of the iterative procedure, used to find whether a contact occurs or not, depends also on the distance computation algorithm chosen. Since distance computation is necessary for all contact algorithms, it is not the purpose of the present article to assess this particular aspect of the performance.

4. NUMERICAL EXAMPLES

Two dynamic contact examples are presented in this section. The first one is a collision between two identical rods. This is a representative example which has been treated, at least, in three articles [5, 10, 11]. In this case, an analytical Poisson function is available and used to test the contact algorithm. A comparison is made between analytical and numerical results . The second example deal with a three-dimensional contact between two disk-shaped elastic bodies that exhibits nonlinear characteristics.

[9] Here δ is the Kroeneker symbol

4.1. Impact between identical rods

Two identical rods, one initially stationary and the other moving with constant velocity $v = 1$ unit, come into contact at time $t = 0$ (see figure 3). The material and geometric properties for each rod are

- density $\rho = 1$ unit,
- cross-sectional area $A = 1$ unit,
- length $L = 10$ unit,
- Young's modulus $E = 1$ unit
- Poisson's ratio $\nu = 0$

4.1.1. Analytical results

For a rod of length L, the analytical Neumann Poisson function giving the displacement at point $x \in [0, L]$ that follow an impact at $x = 0$ and $t = 0$ is

$$N(0,x;t) = \frac{1}{\rho c}\left[Y(t-\frac{x}{c}) + \sum_{k=1}^{+\infty} Y(t+\frac{x-2kL}{c}) + Y(t-\frac{x+2kL}{c})\right]$$

where $c = \sqrt{\frac{EA}{\rho}}$ is the wave velocity in the rod (see Ref. [27]). In this case $c = 1$ unit. A time discretization of this analytical Poisson function and its time derivative, represented in figure 4(i), are used in the contact algorithm with a sample rate set to 100 Hz. The displacements, velocities and contact pressure, plot in figures 5(i) and 5(ii), fit the plots found in Taylor and Papadopoulos [10].

4.1.2. Numerical results

The rod is modeled by two-node, one-dimensional, linear elastic elements. A uniform mesh of 100 elements is considered and the sample rate is also set to 100 Hz. The two numerical Poisson functions (displacement and velocity), plot in figures 4(ii) and 4(iii), differ essentially from analytical ones (Fig. 4(i)) since they are computed using normal-mode expansion (20) with a number of modes restricted to the number of elements in the rod (i.e. 100). This truncation, in the infinite modal series, produces oscillations where accurate dicontinuities should exist (at time $t = 0$, $t = 20$ s, $t = 40$ s etc).

These numerical Poisson functions are used in the contact algorithm and the results are ploted in figure 5(iii) and zoomed in figure 5(iv). The Velocity artefacts are linked to the modal truncation. It is then clear that the errors seen in the numerical solution are correlated to the numerical approximations of the Poisson functions independently of the contact algorithm.

Table 1: Material and geometric characteristics for the three-dimensional numerical example

	Elastic disks
Density	$\rho = 11.3\ 10^3$ Kg.m^{-3}
Young's modulus	$E = 10.4\ 10^6$ Pa
Poisson's ratio	$\nu = 0.37$
Dimensions	$R_{out} = 0.05$ m
Thickness	$e = 5\ 10^{-3}$ m
Initial gap	$h = 0.01$ m
Initial velocities (disk1)	$V_0 = 1$ m.s^{-1} and 6 m.s^{-1}

4.2. Three-dimensional numerical example

For curved contact surfaces, the unilateral behavior on the boundaries may have a substantial influence on the response of the structures: the structural systems, even in cases of linear elasticity and small deformations, exhibits nonlinear characteristics. A collision between two elastic disks is considered here as an illustration of such a phenomenon. An elastic disk, subjected to gravity, is dropped with two different initial velocities ($V_0 = 1$ m.s^{-1} and 6 m.s^{-1}) on an other disk clamped on its edges (see fig. 6). For each initial velocity, the contact algorithm uses the material and geometric characteristics given in table 1 to predict the temporal evolution of the two bodies by computing the distributed contact pressure.

The figures 7 and 8 help to see the spatial pressure distribution on the contact surface. The nodes on the candidate contact surface of the ring are numbered from 1 to 17 according to Fig. 6. The contact surface extends itself for increasing impact velocity and provides a different behavior of the solids.

5. DISCUSSION AND CONCLUSION

This work state a well-posed contact problem by taking into account the balance laws postulated in continuum mechanics. As a consequence in addition to the classical static contact condition, a dynamic condition, already postulated by Taylor [10] and Laursen [11], has been obtained *from* the fundamental physical principles and expresses the way the energy is dissipated during contact. This result contribute to a better basic understanding of contact constraints in the dynamic context. In addition, this condition, used here in a frictionless context, is still true for frictional contact problems. The perspective of this work is to extend this study to dynamical contacts with friction where both tangential and normal tractions have to be determined. To our knowledge this problem is still open.

As mention by Talaslidis and Panagiotopoulos [8], due to unilateral constraints, the estimation of the eigenvalue and eigenvector of the overall system is not possible. Nevertheless, in the present article and within the infinites-

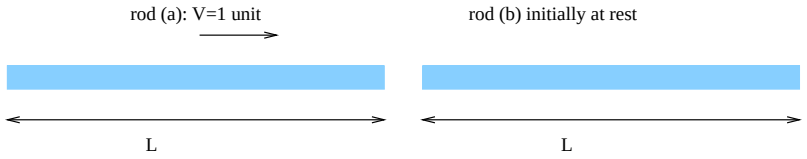

Figure 3: Two identical rods, one initially stationary and the other moving with constant velocity $v = 1$ unit, contact each other at time $t = 0$.

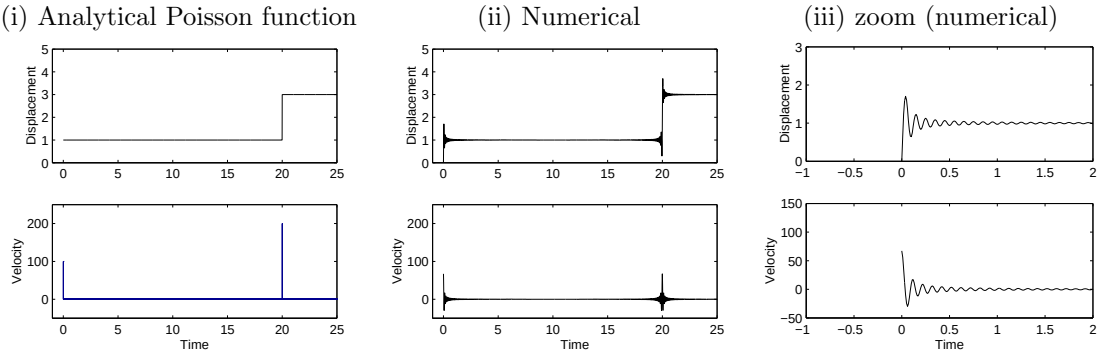

Figure 4: (i) Time discretization of the analytical Poisson functions valid for rod (a) or (b). (ii) Numerical Poisson functions computed using normal-mode expansion and zoomed in subfigure (iii).

imal deformation theory, semi-analytical Green (or Poisson) functions are computed using individual mode expansion for each body. The treatment of wave propagation in the solids is then disconnected from the contact problem by itself and the reciprocal formulation is used in numerical computations reducing the number of unknown and giving a stable solution. As the first numerical example shows, the prediction capacity of the contact algorithm is restricted to the numerical quality of the Poisson function. Since this function is pre-processed, the computational time to solve the contact algorithm remain constant for any desired degree of approximation. Dissipative Green and Poisson functions arising from viscoelastic unconstrained problem are also considered in the contact algorithm. The result is a dissipative system with a dissipative-less contact. At this point, it is important to mention that this method is only applicable to small strain elasticity problems where Green functions make sense. But the Green function can be considered as the first-order term of Volterra kernels expansion, and investigations are done to extend this algorithm to non-linear elastodynamic using Volterra series.

The possibility to predict, with a reasonable computing time, the sound produced by the interaction of two elastic bodies irrespective of the material constitution and geometry constitute the major interest of this study.

A. APPENDIX

A.1. Energy dissipation during contact

Here under is an example to show that the variational statement (4) or, equivalently (7) is not well-posed since several solutions can be obtained. This appendix emphases the fact that any physically relevant solution of the contact problem has to be found by explicitely adressing the energy equation.

Let us take the simple example of a rigid body, of mass m, dropped from altitude h on a rigid foundation. In absence of strain, the variational formulation (7) is reduced to

$$\begin{aligned} &\text{find } (\mathbf{u}, \sigma_n) \text{ such that} \\ &m\ddot{\mathbf{u}} \cdot \mathbf{v} = \mathbf{P} \cdot \mathbf{v} + \sigma_n \cdot v_n \qquad \forall \mathbf{v} \qquad (35a) \\ &(p_n - \sigma_n) \cdot u_n \geq 0 \qquad \forall p_n \leq 0 \qquad (35b) \end{aligned}$$

where $P = mg$ is the weight of the solid and g the gravity constant. Figure 9 represents two possible configurations (trajectory, velocity) corresponding to two types of interaction between the body and the foundation.

case (a) The interaction force is an impulse force acting at time $t = t_c$ of magnitude $2mv_0$

$$\sigma_n(t) = 2mv_0\delta_{t_c}, \quad v_0 = -\sqrt{2gh}, \quad t_c = \sqrt{\frac{2h}{g}}$$

where v_0 is the velocity just before the impact time $t = t_c$ and δ the Dirac distribution. No dissipation occurs in this case.

case (b) The interaction force is also an impulse force but its magnitude is half the one of the first case. After time t_c, the interaction force remains constant and represents the weight of the body

$$\sigma_n(t) = mv_0\delta_{t_c} - Y(t - t_c)P.$$

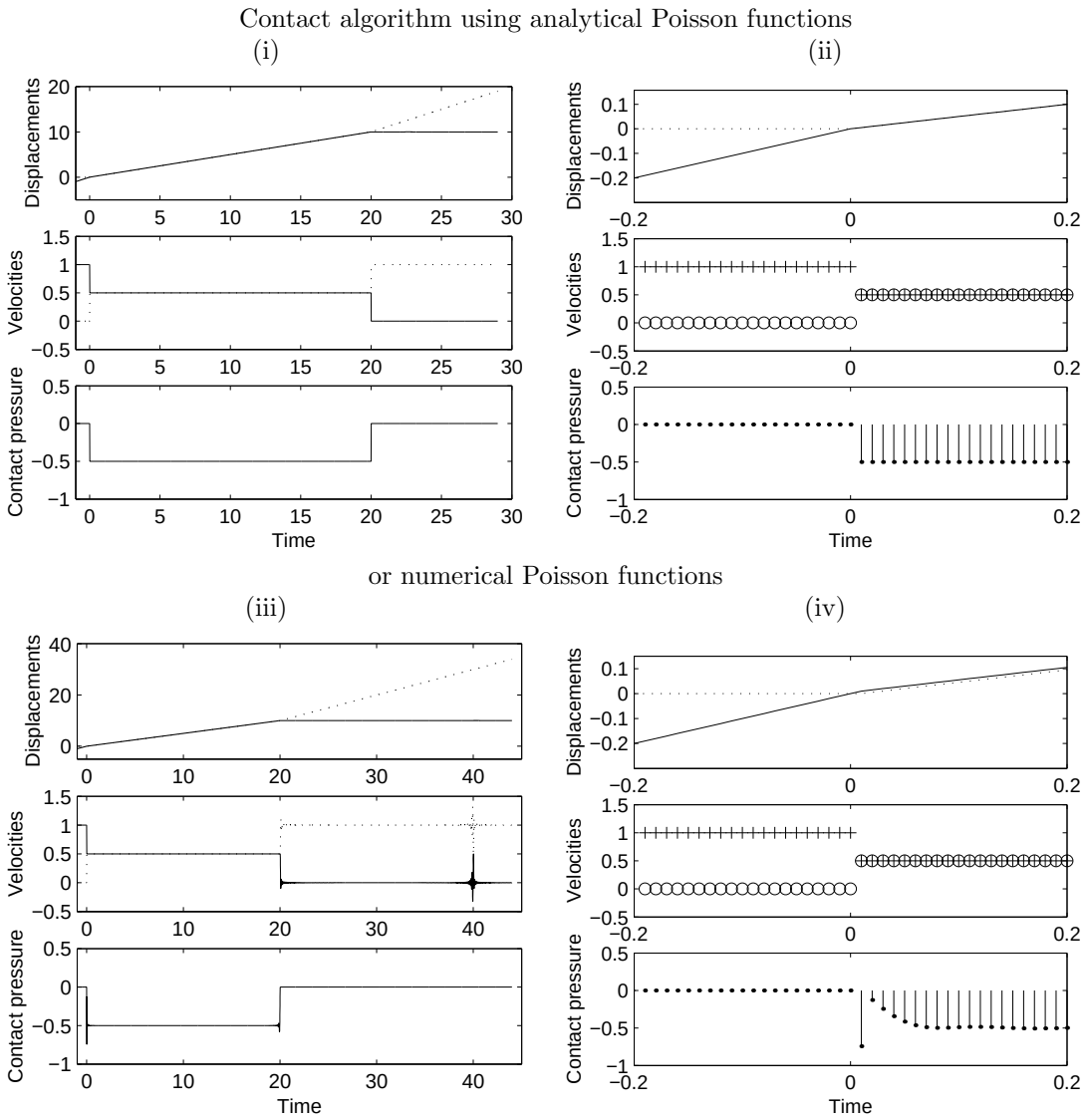

Figure 5: Impact of identical rods. Subfigure (i) : contact algorithm predictions using analytical Poisson functions. Displacements, velocities and contact pressure at contact point of rod (a) (solid line) and rod (b) (dotted line). (ii) First 200 millisecond of interaction. In this model, the contact pressure σ_n is postulated to be a succession of impulse forces. (iii) Impact modeled by finite element method using numerical Poisson functions. The wave reflection at time $t = 20s$ and $t = 40s$ creates artifacts in the velocities. (iv) First 200 millisecond of interaction. A small penetration is observed in the displacement curves.

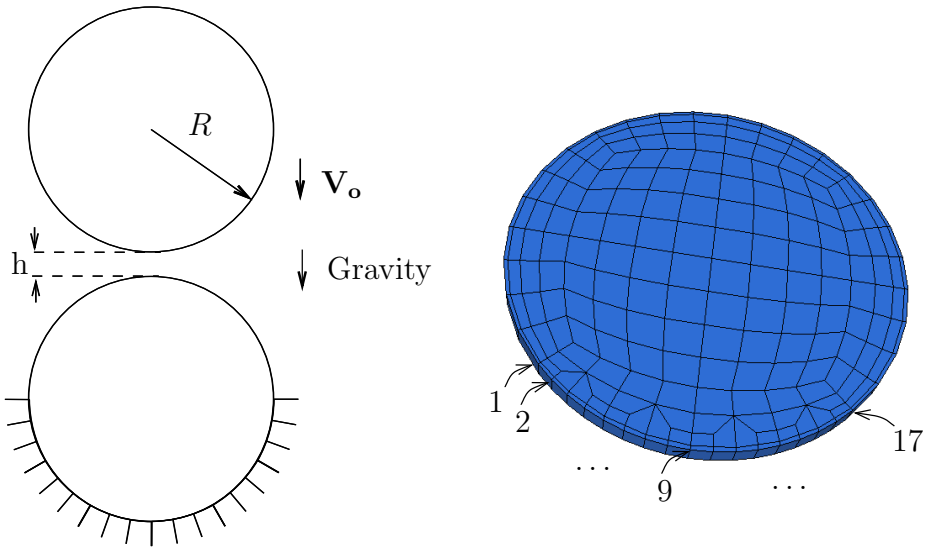

Figure 6: An elastic disk is dropped on an other one clamped on its lowered hemisphere edges. The candidate contact nodes are numbered from 1 to 17.

Here Y is the Heaviside function. The kinetic energy is completely lost at the first contact, and then, the energy is dissipated.

In both cases, the momentum conservation, stated by the variational formulation (35a), is satisfied in the sense of distributions. Moreover, since the product $\sigma_n u_n$ is always null, the formulation (35b) is also checked (note that, the unit vector is directed, as it must be, toward the foundation). In fact, an infinity of solutions exists between these two configurations depending on the way the energy is dissipated during impacts.

A.2. Aknowledgements

The authors would like to thank J. Ferreira, N. Joly, O. Thomas, M. Bruneau, C. Vergez and D. Rocchesso for interesting discussions about this work, as well as N. Ellis for proofreading.

References

[1] A. Signorini. Sopra alcune questioni di elastostatica. In *Atti della Societa Italiana per il Progresso delle Scienze*, 1933.

[2] A. Signorini. Questioni di elasticità nonlinearizzata e semi linearizzata. In *Rend. de Matematica*, Rome, 1959.

[3] G. Fichera. Unilateral constraints in elasticity. In *Actes Congrès Int. Math.*, volume 3, pages 79–84, 1970.

[4] N. Kikuchi and J.T. Oden. *Contact Problems in Elasticity: A Study of variational Inequalities and Finite Element Methods*. Siam, Philadelphia, 1988.

[5] T.J.R. Hughes, R. L. Taylor, J. L. Sackman, A. Curnier, and W. Kanoknukulchai. A finite element method for a class of contact-impact problems. *Computer Methods in Applied Mechanics and Engineering*, 8:249–276, 1976.

[6] G. Duvaut and J.L. Lions. *Les inéquations en mécanique et en physique*. Dunod, Paris, 1972.

[7] J.A.C Martins and J.T. Oden. A numerical analysis of a class of problems in elastodynamics with friction. *Computer Methods in Applied Mechanics and Engineering*, 40:327–360, 1983.

[8] D. Talaslidis and P. D. Panagiotopoulos. A linear finite element approach to the solution of variational inequalities arising in contact problems of structural dynamics. *International Journal for Numerical Methods in Engineering*, 18:1505–1520, 1982.

[9] H. Antes and P. D. Panagiotopoulos. *The boundary integral approach to static and dynamic contact problems : equality and inequality methods*. BirkhAuser, Basel ; Boston, 1992.

[10] R.L. Taylor and P. Papadopoulos. On a finite element method for dynamic contact/impact problems. *International Journal for Numerical Methods in Engineering*, 36:2123–2140, 1993.

[11] T.A. Laursen and V. Chawla. Design of energy conserving algorithms for frictionless dynamics contact problems. *International Journal for Numerical Methods in Engineering*, 40:863–886, 1997.

[12] Y. Ayyad, M. Barboteu, and J.R. Fernández. A frictionless viscoelastodynamic contact problem with energy consistent properties: Numerical analysis and computational aspects. *Computer Methods in Applied Mechanics and Engineering*, 198:669–679, 2009.

[13] M. Cocou. Existence of solutions of a dynamic signorini's problem with nonlocal friction in viscoelasticity. *Zeitschrift für Angewandte Mathematik und Physik (ZAMP)*, 53(6):1099–1109, 2002.

[14] P. Deuflhard, R. Krause, and S. Ertel. A contact-stabilized newmark method for dynamical contact problems. *International Journal for Numerical Methods in Engineering*, 73(9):1274–1290, 2008.

[15] P.G. Ciarlet. *Introduction à l'analyse numérique matricielle et à l'optimisation*. Masson, Paris, 1990.

[16] A.C. Eringen and E.S. Suhubi. *Elastodynamics*, volume I-finite motions. Academic Press, New York, 1975.

[17] P. Germain. *Cours de Mécanique des milieux continus*. Masson, Paris, 1976.

[18] J. Salençon. *Mécanique des milieux continus*. Ellipse, Paris, 1988.

[19] M. Bruneau. *Manuel d'acoustique fondamentale*. Hermes, Paris, 1998.

[20] Joël Bensoam. *Représentation intégrale appliquée à la synthèse sonore par modélisation physique : méthodes des éléments finis*. Thèse de doctorat, Académie de Nantes Université du Maine, 2003.

[21] T.A. Laursen and J.C. Simo. A continuum-based finite element formulation for the implicit solution of multibody, large deformation frictional contact problems. *International Journal for Numerical Methods in Engineering*, 36:3451–3485, 1993.

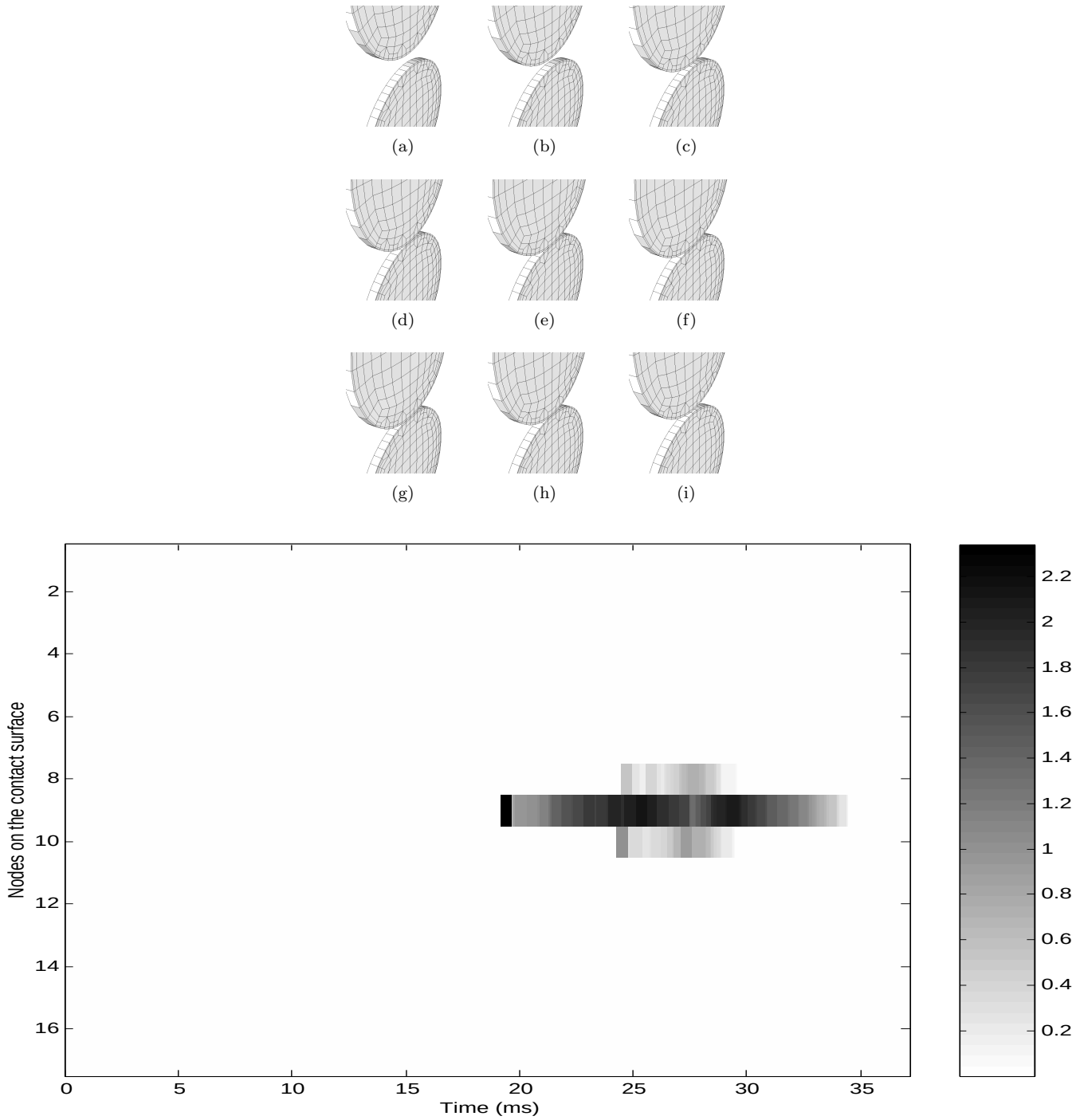

Figure 7: Nine snapshops of a collision between two disks and contact force (in mPa) excerted on the contact surface for an initial velocity : $V_0 = 1$ m.s^{-1}. The contact surface is localized around the central node 9 and involves exceptionally the node 8 and symetric 10. The ninth node stay in contact.

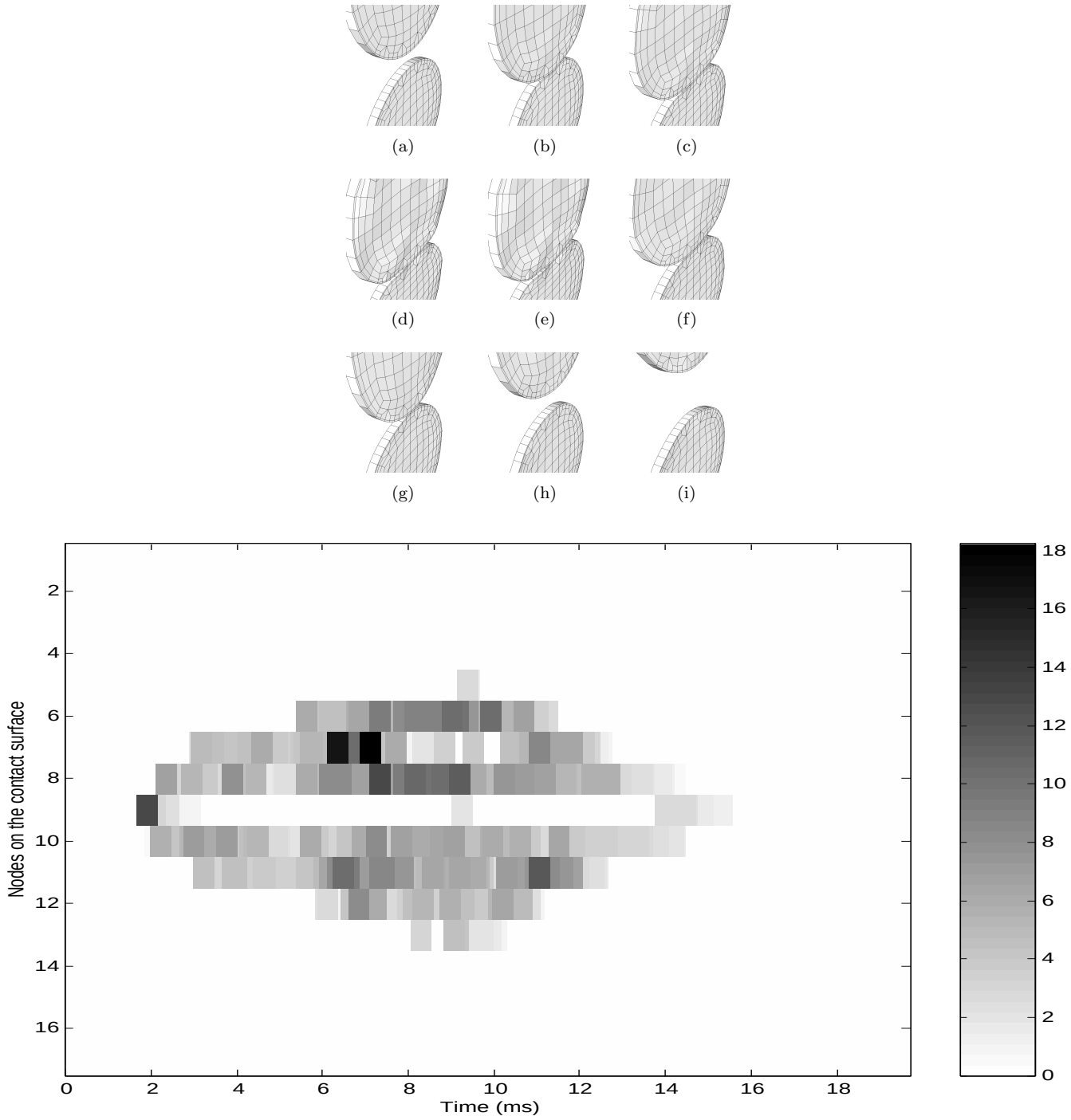

Figure 8: Nine snapshops of a collision between two disks and contact force (in mPa) exerted on the contact surface for an initial velocity : $V_0 = 6$ m.s^{-1}. When the contact surface extends itself beyond the node 8 (and symmetric 10) the ninth node is no longer in contact and a gap appears (compare with figure 7)

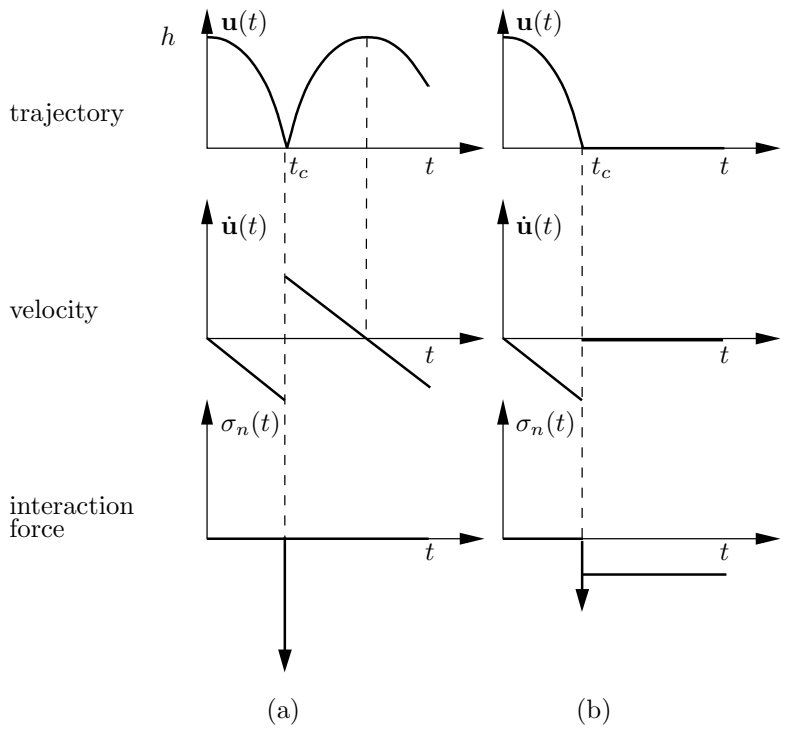

Figure 9: Trajectory and velocity of a rigid body dropped on a rigid foundation for two different interaction forces. Case (a): energy is conserved. Case (b): the kinetic energy is lost at the first contact. This simple example illustrates the non uniqueness of the contact problem if the dynamical contact condition is not imposed.

[22] V. Chawla and T.A. Laursen. Energy consistent algorithms for frictional contact problems. *International Journal for Numerical Methods in Engineering*, 42:799–827, 1998.

[23] V.A. Kozlov, V.G. Maz'ya, and J. Rossmann. *Elliptic boundary value problems in domains with point singularities*. American Mathematical Society, Rhode Island, 1997.

[24] J. Bensoam, N. Misdariis, C. Vergez, and R. Caussé. Formulation intégrale et technique des éléments finis appliquées à la synthèse sonore par modèles physiques : Représentations intégrales utilisant la fonction de green et le noyau de poisson. In *CFA : Congrès Français d Acoustique*, Lille, France, 2002. SFA. paper to appear.

[25] A.C. Eringen and E.S. Suhubi. *Elastodynamics*, volume II-linear theory. Academic Press, New York, 1975.

[26] J. Bensoam, C. Vergez, N. Misdariis, and R. Caussé. Formulation intégrale et technique des éléments finis appliquées à la synthèse sonore par modèles physiques. In *XVème Congrès Français de Mécanique*, number 453, Nancy, 2001. CFM.

[27] K. F. Graff. *Wave Motion in Elastic Solids*, chapter 2. Dover Publications, Inc., New York, 1975.